DEVELOPING AND ESTABLISHING A PLATFORM FOR THE AUTOMATION OF MONOCLONAL ANTIBODY DRUG ANALYSIS

By
Joseph Federico

A thesis submitted to the Johns Hopkins University in conformity with the requirements for the degree of Master of Science in Engineering.

Baltimore, Maryland
October 2018

ABSTRACT

The use of automation has been standardized for generations in many industries, ranging from car manufacturing to oil refinery, and continues to advance at a rapid pace. While the power of automation has been harnessed in many other industries, the biotechnology sector has lagged behind, largely due to the complexity of working with biological matter as well as the complexity and the ever-changing nature of the processes involved.[1] In recent years, the automation trend has gained in popularity in the field of biotechnology and many companies are seeking to utilize the new instruments and technology available to increase efficiency as well as optimize many other characteristics of their processes.

Automation has the potential to significantly increase the overall productivity of a biopharmaceutical company by strategically implementing it where workflow traditionally slows due to bottlenecks, such as in analytical departments. Yet, in addition to improving efficiency, automation offers the unique ability of improving reproducibility and decreasing variation by transferring repetitive tasks to a robot. The elimination of human error and the ability to track all robotic movements well suits the ultimate goal of producing a high-quality product, which is of utmost importance in a good manufacturing practices (GMP) compliant environment.

Currently, the standard for analyzing developmental drug samples is either by manually performed assays or on instruments dedicated to a particular assay. Therefore, we developed a customizable and versatile automated platform to replace a range of existing manual assays that test varying aspects of a monoclonal antibody drug sample.

In this study, we used the Hamilton Microlab STAR robot to automate two relative drug potency assays and one residual Chinese Hamster Ovarian (CHO) host cell protein (HCP) assay. For all assays, all liquid handling steps are automated and performed by the robot. In this essay, we demonstrate that our automated assays can achieve equal or superior accuracy and precision compared to their manual counterparts, have a greater maximum efficiency, and track and record all robotic movements performed during the assay. Furthermore, our work establishes a precedent upon which future assays can be more easily translated into an automated environment.

PREFACE AND ACKNOWLEDGEMENTS

The work presented in this Master's Essay was performed over the course of a 27-week cooperative internship at MedImmune, LLC., a wholly owned subsidiary of AstraZeneca, in conjunction with the Institute for Nanobiotechnology at The Johns Hopkins University. As a part of the AstraZeneca family, MedImmune focuses on developing biologics for three core areas of therapy: oncology; respiratory, inflammation and autoimmune; and cardiovascular and metabolic disease. This essay does not divulge any names or mechanisms of action of any drug manufactured by MedImmune or AstraZeneca as the work performed does not directly involve this. Therefore, in order to best maintain the confidentiality of MedImmune and its work, any references to particular drugs have been removed and replaced with a numbering system.

There are many people at MedImmune I would like to thank who helped bring this work to fruition. Dr. Veerendra Koppolu oversaw and helped guide me throughout this entire project. Craig Lamison is responsible for all the computer coding needed for this project. Jonathan Borman also oversaw and directed this project while also developing the initial sample data processing required for certain assays. Additionally, Elizabeth Shrout is also responsible for a significant amount of the initial development work done on the first relative potency assay presented in this essay.

I would also like to thank the Johns Hopkins community, including Tom Fekete for organizing and maintaining this academic-industrial relationship. Finally, I would like to extend my most sincere thanks to Dr. Sharon Gerecht for affording me this opportunity in my Master's degree as well as for being a trusted advisor and mentor over the past four years.

TABLE OF CONTENTS

ABSTRACT ..... **II**

PREFACE AND ACKNOWLEDGEMENTS ..... **III**

1 INTRODUCTION **1**

2 MATERIALS AND METHODS **2**

2.1 Robotic System and Incorporated Instruments 2
2.2 Critical Reagents 3
2.3 Cell Culture 3
2.4 Potency Assay Automation Protocol 4
2.5 Residual CHO HCP Automation Protocol 7
2.6 Data Analysis and System Suitability 10

3 RESULTS **12**

3.1 Relative Potency Assays 13
3.2 Residual CHO Host Cell Protein Assay 17

4 DISCUSSION AND FUTURE DIRECTIONS **24**

5 CONCLUSION **27**

6 REFERENCES **28**

7 APPENDIX: SUPPLEMENTAL DATA **29**

LIST OF TABLES

Table 1: System Suitability for Potency Assays 11

Table 2: Europium Standard Curve Tested as Simulated Samples 20

Table 3: Drug Potency Assay 1 Data 29

Table 4: Drug Potency Assay 2 Data 29

LIST OF FIGURES

Figure 1: Layout of Hamilton STAR Liquid Handling Robot for a General Potency Assay. 4
Figure 2: Staggered Row Plating of Potency Samples. 5
Figure 3: General Potency Assay Procedure at the Molecular Level. 6
Figure 4: Hamilton Microlab STAR Deck Layout for the Residual CHO Host Cell Protein Assay. 7
Figure 5: Dilution Scheme for up to 36 Host Cell Protein Samples. 8
Figure 6: Residual CHO Host Cell Protein Assay Plate Layout. 9

Figure 7: CHO Host Cell Protein Assay at the Molecular Level. 10
Figure 8: Diagram of Overall General Automated Bioassay. 12
Figure 9: Accuracy of Simulated Potency Samples. 14
Figure 10: Precision of Simulated Potency Samples. 14
Figure 11: Linearity of Simulated Samples. 15
Figure 12: Ratio of Means of Manual vs. Automated Methods. 17
Figure 13: Dynamic Range of HCP Assays. 18
Figure 14: Linearity of Standard Curves. 19
Figure 15: Accuracy and Precision of the Manual Europium HCP Assay. 20
Figure 16: Linearity of Manual Europium HCP Assay. 21
Figure 17: Accuracy and Precision of Upper and Lower Limits of Automated HCP Europium Assay. 22
Figure 18: Normalized Linearity of 1:2 Dilutions. 23
Figure 19: Accuracy and Precision of Simulated HCP Samples with Additional CHO Impurities. 24
Figure 20: DOE for Establishing a Residual CHO HCP Assay using DELFIA Europium. 30

1 INTRODUCTION

Critical to the research and development of biopharmaceuticals is the continuous and periodic analysis performed to characterize a drug product throughout its developmental progression. A wide variety of analytical methods are employed to better understand a given product and can measure many aspects of a drug such as drug concentration, drug potency, impurity identification and concentration, as well as other physical properties of the molecule. Our increasing understanding of the complex nature of biopharmaceutical products as well as their continual growth in the therapeutic market has resulted in an ever-growing demand for developmental analysis.[2] This increased demand has created in many analytical departments a bottleneck at which analysts are overwhelmed despite working at maximum efficiency. This subsequently results in the slowing of all developmental work for which decisions are made based upon the results of analytical testing. The implementation of automation offers an opportunity to mitigate this bottleneck with its potential to increase efficiency capable of high throughput analysis.

Laboratory automation of standard protocols is one effective method for increasing high throughput efficiency. However, increased efficiency is only one of the many possible benefits of implementing laboratory automation. The use of a robot to replace a human analyst has the benefit of programmed consistency and elimination of human error. Humans are prone to make mistakes, especially after a series of repetitive manual maneuvers from repeating similar assays. A robot is far less prone to mistakes. Furthermore, while a robot is not immune to errors, automation also comes with the added benefit that every step in an assay is recorded, a desirable feature especially for good manufacturing practices (GMP) compliant environments. Additionally, when programmed appropriately, a robot should perform the same task in the same way every time, giving a robot unique consistency that is difficult to achieve with a single analyst, let alone between multiple analysts and across departments.

Immunoassays are one of the most common analytical methods due to their high specificity and sensitivity, which allow for a reliably accurate and precise method of measurement. One of the most frequently used immunoassays is the Enzyme Linked Immunosorbent Assay (ELISA). While the ELISA is effective and reliable, its long preparation and incubation times as well as rigorous and repetitive liquid handling steps result in a low threshold for maximum efficiency.[3]

These characteristics, in addition to the ELISA's generic format for a wide variety of assays, make the ELISA a good candidate for automation with liquid handling robots.

In this study, ELISA-based assays were modified from their original manual protocols and automated using a Hamilton Microlab STAR Liquid Handling Robot. One of the most foundational assays for a drug quantitatively measures its biological activity, also known as drug potency. In this study, two cell-based ELISAs were automated to measure the relative potency of monoclonal antibody drug substance, in which both drugs of interest target and bind cell surface ligands. Additionally, as monoclonal antibody drugs are produced in mammalian cells and subsequently purified, downstream processing of these samples requires the routine analysis of impurities from the host cell in which it was produced, including what are known as host cell proteins (HCPs). To this end, we modified an existing manual ELISA that measures residual host cell protein in drug produced in CHO cells and simultaneously developed an automated protocol for it. While the general procedure of an ELISA is straight forward, each assay requires a complex scheme for properly diluting each submitted sample.

We present three automated ELISA-based assays in this report, two measuring relative potency and one measuring residual CHO HCP. For each assay, an analyst prepares coated microtiter plates, reagents, and samples and loads them onto the robot, which automatically calculates and performs all dilutions as well as incubation and washing steps. In addition to liquid handling steps, all data analysis, including results and system suitability validity checks, is automated.

2 MATERIALS AND METHODS

2.1 Robotic System and Incorporated Instruments

For all automated experiments in this study, a Hamilton Microlab STAR workstation (Hamilton Company, Reno, Nevada) was customized and coded to perform the liquid handling steps of the ELISAs on 96-well microtiter plates. The workstation was outfitted with an eight-individual channel head, a 96-channel Probe head, an iSWAP Gripper, and CO-RE Paddle Grippers. A peripheral microplate washer (BioTek ELx405, BioTek, Winooski, Vermont) was incorporated with the workstation; the robot transferred 96-well assay plates to the plate washer using the iSWAP gripper and communicated with the instrument to wash each plate. All samples

prepared automatically were finally analyzed using an Envision Microplate Reader (Perkin Elmer, Waltham, Massachusetts) capable of reading time-resolved fluorescence with excitation at 340 nm and emission at 615 nm. The workstation was customized to a particular set up for both the potency and HCP assays automated in this study, diagrammed in the following sections.

2.2 Critical Reagents

All critical reagents across all studies were qualified to internal company standards. Critical reagents for each potency assay included the respective cell line, the control, reference standard, and the DELFIA® Eu-N1 Anti-Human IgG (Perkin Elmer, Waltham, Massachusetts). In order to maintain consistency of relative potency measurements in the potency assays of this study, all samples (reference standard, control, and simulated potency samples) were taken from the same qualified drug substance lot. Simulated potency samples were dilutions of the same material with concentrations of 60%, 77%, 130%, and 167% relative to the control and reference standard concentrations.

The residual host cell protein assay required the polyclonal capture antibody, the CHO HCP antigen standard, the CHO HCP antigen control, the biotinylated anti-CHO antibody, and DELFIA® Eu-N1 Streptavidin conjugate (Perkin Elmer, Waltham, Massachusetts). In the development experiments in this study, HCP antigen standard qualified material was used for the standard curve as well as the control and simulated samples to test for the assay's ability to accurately determine HCP concentration.

2.3 Cell Culture

Each potency cell-based ELISA required a different cell type. For Potency Assay 1, P0 HepG2 cells were thawed and cultured in DMEM supplemented with 10% FBS and 1% NEAA. Cells were passaged twice after reaching 80-90% confluency. After two passages, HepG2 cells were plated into the inner 60 wells of three Corning® PureCoat™ Amine, Black/Clear Flat Bottom 96-well plates (VWR, US) at 150,000 cells/well in 100 µl of media. Plates were then incubated at 37±2°C with 5±1% CO_2 and greater than 85% relative humidity for 20±1 hours. After this incubation, plates containing HepG2 cells were allowed to equilibrate to room temperature on the deck of the Hamilton STAR robot.

In contrast to culturing cells for two passages, Potency Assay 2 used Assay Ready Banks (ARBs) of frozen CHO-K1 cells. While Potency Assay 1 required culturing of HepG2 cells for two passages, ARBs for Potency Assay 2 were frozen such that they can be directly added to assay plates upon thaw. Therefore, each ARB was thawed and plated into the inner 60 wells of three Corning 96-well poly-D-lysine coated flat bottom plates (VWR, US) at 40,000 cells/well in 100 µl of assay media (same media as Potency Assay 1). Plates were then placed in an incubator overnight at 37±2°C with 5±1% CO_2 and greater than 85% relative humidity for 21±5 hours. After incubation, plates equilibrated to room temperature while on the deck of the robot.

2.4 Potency Assay Automation Protocol

All reagents necessary for the experiment, as well as samples, dilution blocks, tips, and sample plates are loaded onto the deck of the Hamilton STAR liquid handling robot at the beginning of the procedure. The automated protocol for each potency assay can test up to 12 samples in triplicate. In comparison to the manual method, one assay is assumed to mean 4 samples tested in triplicate performed in three plates with staggered row plating.

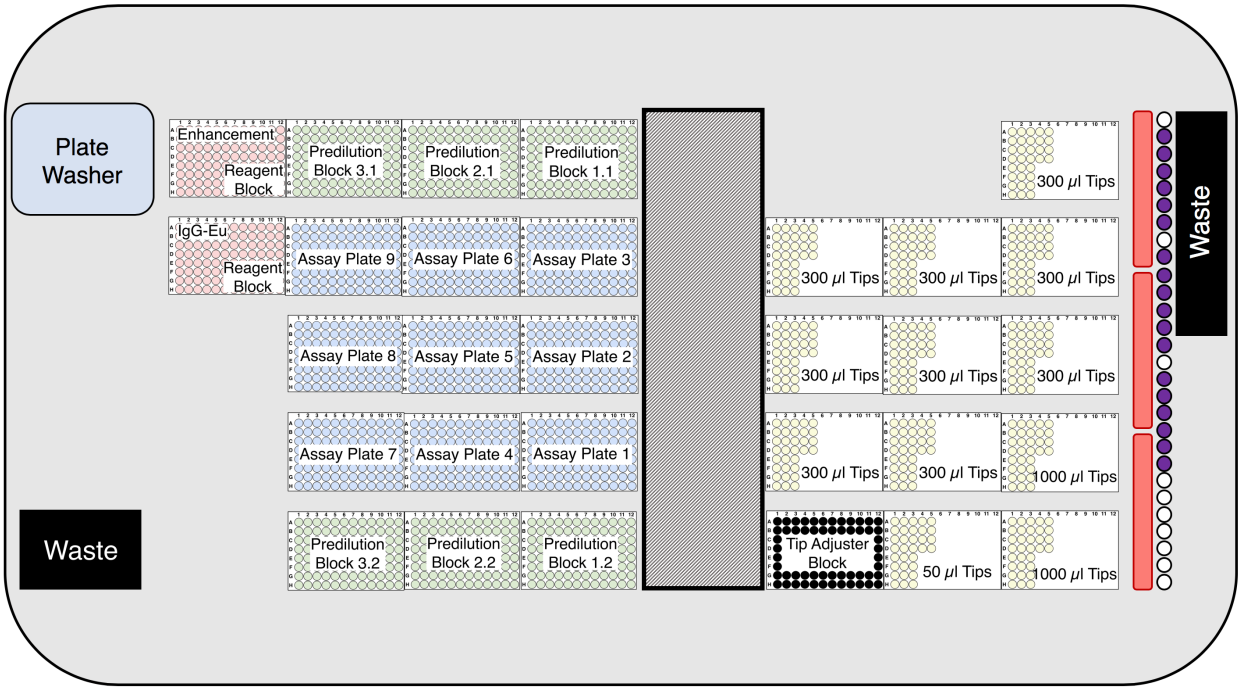

Figure 1: **Layout of Hamilton STAR Liquid Handling Robot for a General Potency Assay**.

The diagram displays where each item, including assay plates, deep well blocks, reagents troughs, etc., is placed on the deck of the robot during a general potency assay. The tip adjuster block is required for the staggered row plating

of the samples that is explained in Figure 2. The purple and white circles to the right indicate a rack that holds microcentrifuge tubes: the purple circles represent a microcentrifuge tube that is occupied by a sample, reference standard, or control. The gap in the middle of the deck is necessary for the arm of the robot that picks up each assay plate and transports it to the plate washer to have enough room to access assay plates 1-3. The waste in the top right of the desk is for tips used by the eight-channel head while the one in the bottom left is for tips used by the 96-channel head.

The Hamilton software that controls the robot directs the analyst through the placement of each item on the deck of the robot. When prompted to place the samples on the deck of the instrument, the user is prompted to enter the concentration of each sample. In the first predilution block, the robot uses these values to calculate the appropriate volume of diluent (DMEM supplemented with 10% FBS and 1% NEAA) while maintaining a consistent sample volume to bring the reference standard, control, and samples to a uniform concentration. In the same block, samples are diluted two more times to a final concentration of 24 µg/ml for Potency Assay 1 and 6 µg/ml for Potency Assay 2. In the second predilution block, all samples are transferred from the first block and are then serially diluted nine times 3.2-fold for Potency Assay 1 and 3-fold for Potency Assay 2.

After samples have been prepared by the robot, each assay plate is washed three times in 1x PBS (VWR, US) in the peripheral BioTek ELx405 microplate washer. Wash protocols were optimized to avoid disturbing the adherent cells while also efficiently washing each well; to this end, the first two washes are partial aspirations while the final wash removes all liquid. All wash steps are performed to these specifications.

After washing, 100 µl of each prepared dilution are added to assay plates. Up to 12 samples can be tested at once, with 4 samples being tested in three plates in staggered row triplicates as shown below:

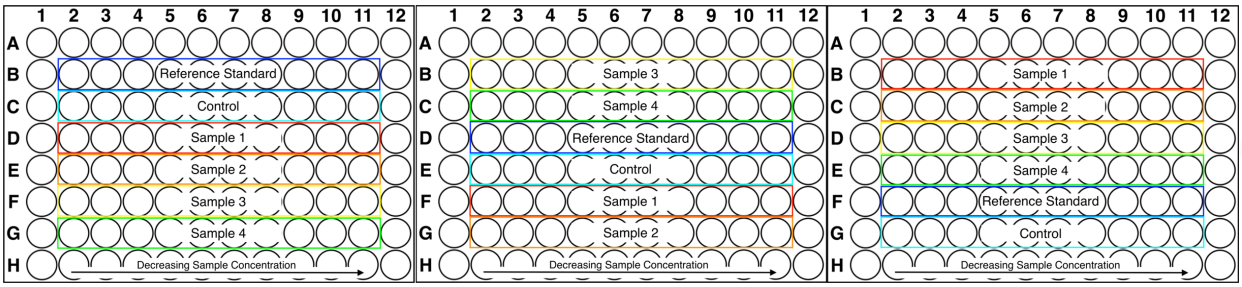

Figure 2: **Staggered Row Plating of Potency Samples**.

For each assay performed automatically, there is a reference standard, control, and up to four samples that are plated in triplicate across three different 96-well plates. The staggered row plating is designed to avoid plate effects that could discriminately affect one sample differently than another. Sample concentrations decrease from left to right and

are prepared by a serial dilution that is performed in Predilution Block 1.2, 2.2, or 3.2 (refer to Figure 1) depending on its placement in the automated assay.

Samples are incubated on the deck of the robot at room temperature, as well as all further incubations, for 40 ±10 minutes (Potency Assay 1) and 50 ±10 minutes (Potency Assay 2). When the incubation is finished, plates are washed three times again in 1x PBS and incubated again in 100 µl/well of 65 ng/ml DELFIA Eu-N1anti-human IgG for 60 ±10 minutes. Plates were washed again and then incubated with 100 µl/well of DELFIA® Enhancement Solution for 45 minutes, after which the plates are manually removed from the deck of the Hamilton robot and read by an EnVision Microplate Reader using time-resolved fluorescence with 340 nm excitation and 615 nm emission.

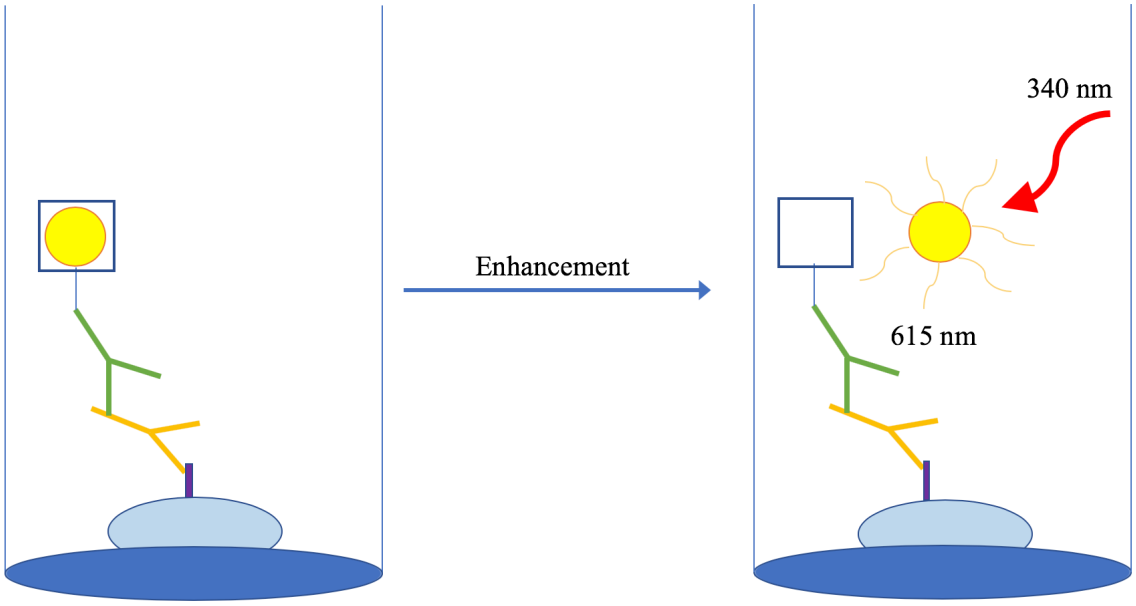

Figure 3: **General Potency Assay Procedure at the Molecular Level**.

The diagram shows a sketch a of what happens at the molecular level during the ELISA procedure. First, cells are coated onto the surface of each well (cells are represented by light blue oval with dark blue circumference). Each cell displays a ligand (purple rectangle) that the drug sample binds. The mAb drug is then bound on its Fc region by a secondary immunoglobulin G antibody that is conjugated to Perkin Elmer's DELFIA Europium. Upon incubation with DELFIA Enhancement solution, the Europium is released and can be activated with absorbance light at 340 nm and emits light at 615 nm.

The figure above presents the general format by which both potency assays operate at the molecular level. Each incubation in the assay represents a different molecule binding the scaffold pictured above, in which the final step involves activating the DELFIA Europium signal.

2.5 *Residual CHO HCP Automation Protocol*

As with the potency assays, all reagents, samples, dilution blocks, tips, sample plates, and other required equipment are loaded at the start of the automated CHO HCP assay as directed by the program. The assay can accommodate up to 36 samples on a total of nine assay microplates.

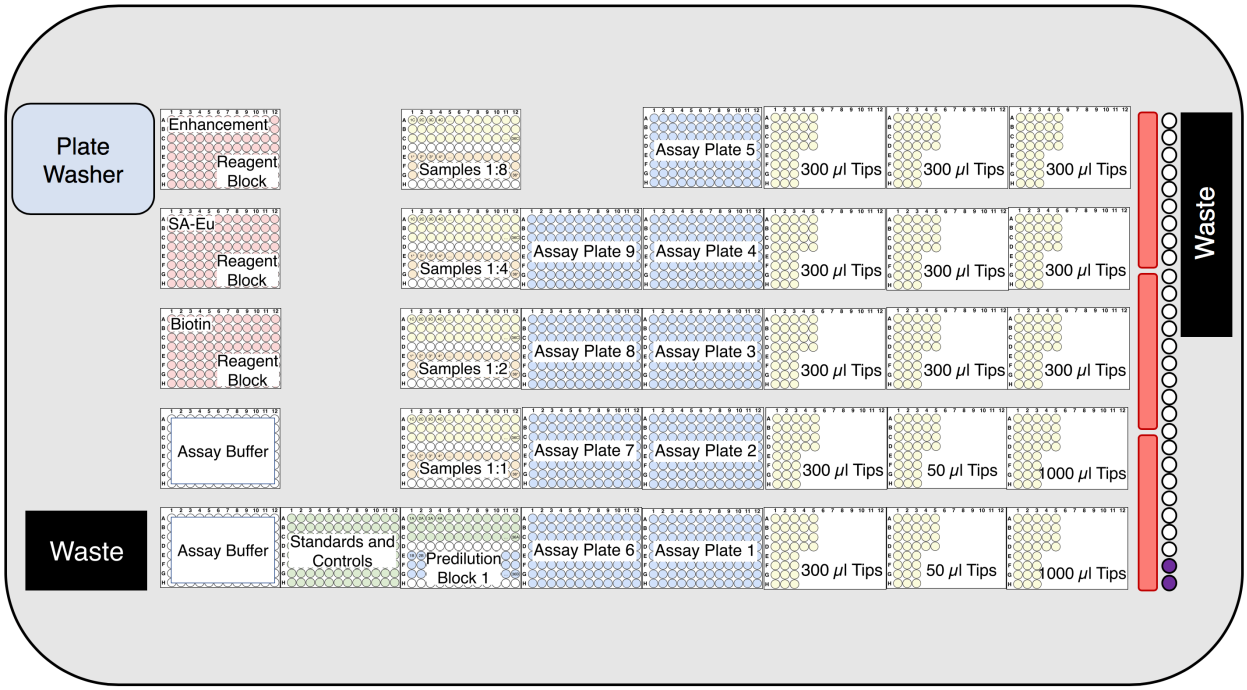

Figure 4: **Hamilton Microlab STAR Deck Layout for the Residual CHO Host Cell Protein Assay**.

The diagram shows where each item involved in the automated ELISA procedure to measure residual CHO HCP sits on the desk of the Hamilton STAR. The two microcentrifuge tubes present represent the stock control and the stock spike solutions.

96-well EIA/RIA clear flat bottom polystyrene high binding microplates (Corning) are coated with 100 µl/well of an in-house polyclonal capture antibody at 4 µg/ml in 1x PBS. Plates are incubated overnight at 2-8°C for at least 16 hours (up to 7 days). After overnight incubation, the plates are allowed to equilibrate to room temperature for 30 minutes on the deck of the Hamilton STAR. After the plates have come to equilibrium, the robot transfers each plate consecutively to the BioTek plate washer where each plate is washed three times in 300 µl/well of 1x PBS/0.05% Tween-20 wash buffer, which is used for all wash steps throughout the assay. After washing, the robot dispenses 250 µl/well of 1% BSA 1xPBS/0.1% Tween-20 blocking buffer/assay diluent and incubates on the deck of the robot for 2 hours. During this time, dilutions of standard curve, control, samples, and sample spikes are performed automatically by the robot. For up to 36 samples of varying impurity concentrations, the Hamilton STAR can efficiently

perform all necessary dilutions during the two-hour incubation, which allows the program to make use of Hamilton's parallel processing, making this assay highly efficient.

During the blocking incubation, the robot first prepares the standard curve and spike solution using stock CHO HCP antigen, the positive control from qualified CHO HCP positive control, and the negative control from assay buffer in a 2 ml deep 96-well block.

The robot then performs dilutions of all samples and sample spikes according to data regarding expected impurity amount that is input by the analyst. Using a preprogrammed hitpick file in Microsoft Excel, the analyst inputs the sample identification number and its corresponding dilution factor ranging from 1:2 to 1:2000 that is estimated based on its expected impurity concentration. The hitpick file generates three .CSV worklists that the robot uses to calculate and perform each sample dilution.

Samples are loaded by the analyst into the top half of a 2 ml deep 96-well block and the robot performs the first dilution into the bottom half of the block and the second dilution into the top half of a second block. After each sample is at the appropriate concentration in the top half of the second block, the robot uses that material and the previously prepared spike material to generate the up to 36 spiked samples in the bottom half of the second block. Spiked samples are spiked with 250 ng/ml antigen by a 90 vol% sample and 10 vol% spiking material (2500 ng/ml).

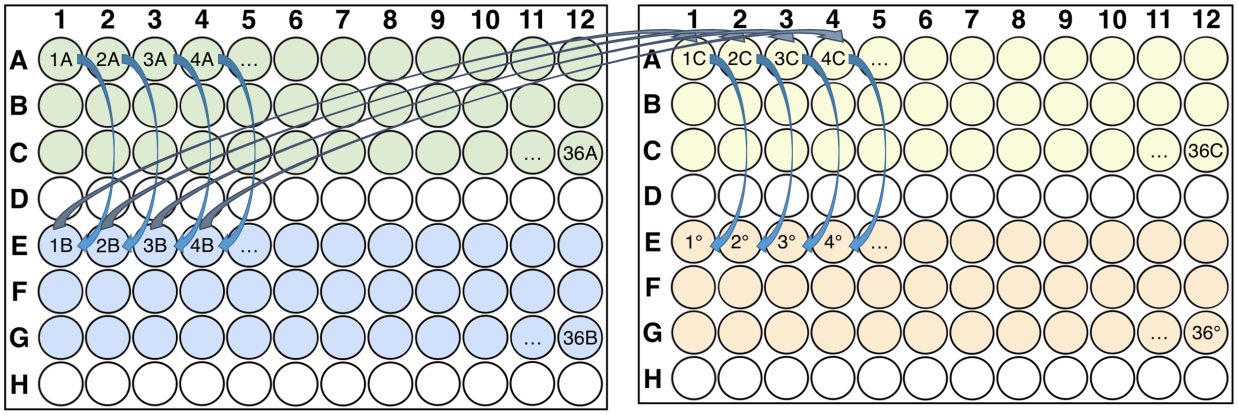

Block 1 Block 2

Figure 5: **Dilution Scheme for up to 36 Host Cell Protein Samples**.

At the start of the assay, the analyst dispenses up to 36 samples in the top half of Block 1, indicated by positions 1A-36A. From this, the robot performs two dilutions to achieve the final sample concentration, starting from the top of Block 1 to the bottom, and then a second dilution from the bottom of Block 1 to the top of Block 2. Then, slightly less than the 1 mL of liquid in each sample in the top of Block 2 (1C-36C) is transferred to the bottom of Block 2 for the spiked samples (1°-36°).

The contents of block 2 above then becomes the starting material for the series of three 1:2 whole plate dilutions performed using the robot's 96-probe head such that each sample, including spikes, is represented by a 1:1, 1:2, 1:4, and 1:8 dilution.

After the two-hour blocking step, the plates are washed three times and the robot then adds the standard curve, samples, sample spikes, and controls in the following pattern:

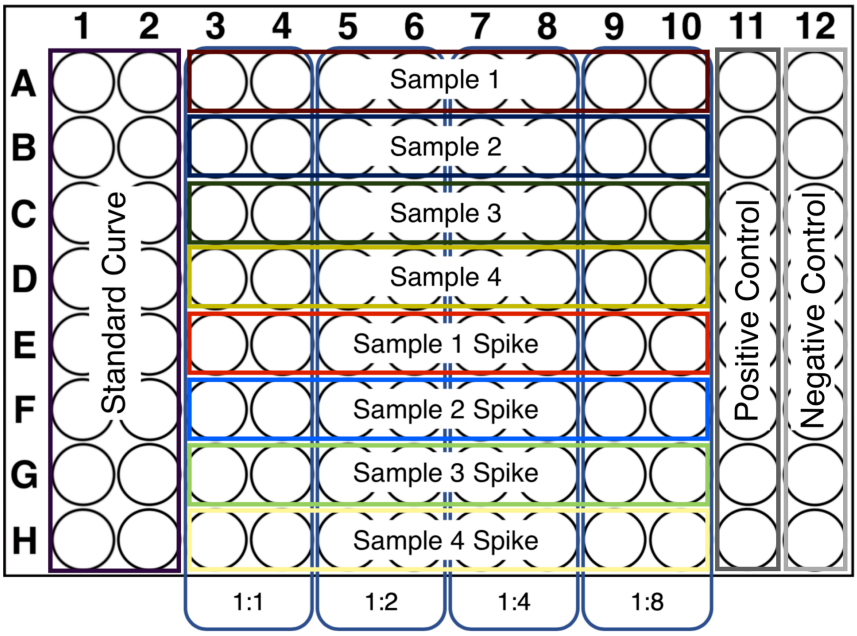

Figure 6: **Residual CHO Host Cell Protein Assay Plate Layout**.

In each assay plate, the standard curve ranges from 4500 ng/ml known HCP to 2 ng/ml and is plated in duplicate. Each sample is represented on the plate in a standard and spiked solution in rows A-H with a series of 1:2 dilutions in columns 3&4, 5&6, 7&8, and 9&10. Positive and negative controls are located in columns 11 and 12.

After the robot is finished dispensing into the first plate (of maximum nine), a timer of 80 minutes is started while the robot finishes the remaining plates. Including the time it takes the robot to plate each sample as well as the time it takes to wash each plate, any given assay plate incubates between 40 and 80 minutes. This range of incubation time was confirmed using a design of experiment study (see Appendix).

The assay plates are washed after the sample incubation and are incubated for 60 minutes in 100 µl/well of in-house biotinylated anti-CHO antibody at 2 µg/ml in assay diluent. Plates are washed three times again, and subsequently incubated in 65 ng/ml of Streptavidin conjugated Europium in assay diluent for 60 minutes. Plates are washed three times, and finally incubated in DELFIA Enhancement Solution for 45 minutes on the deck on the deck of robot. At the end of this

incubation, all nine plates are analyzed on a Perkin Elmer EnVision Microplate Reader using time-resolved fluorescence with 340 nm excitation and 615 nm emission.

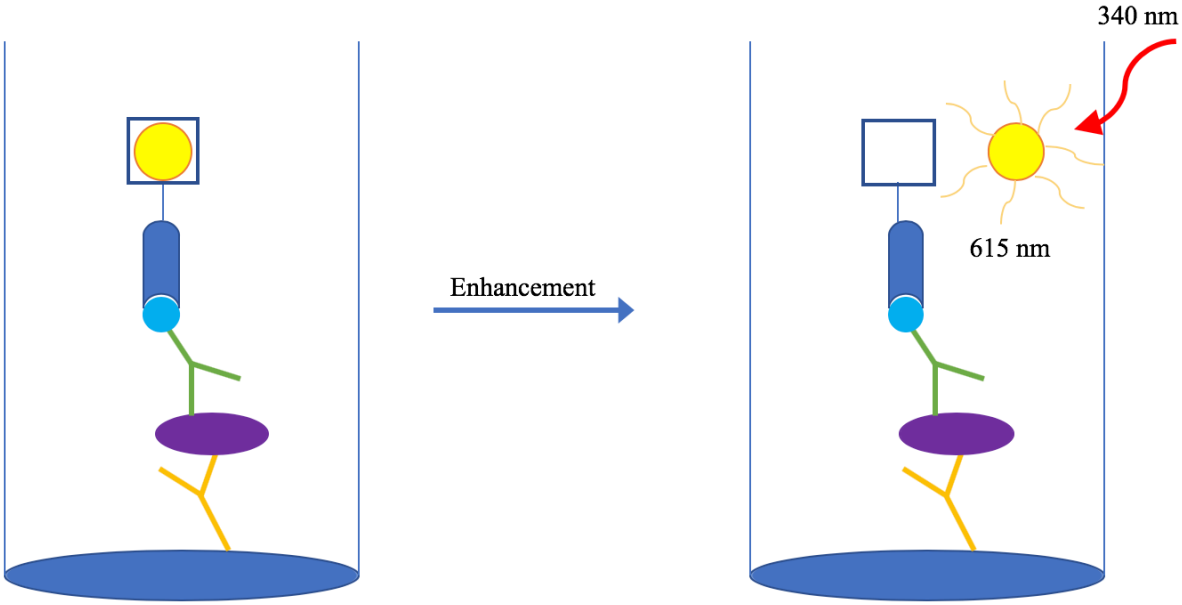

Figure 7: **CHO Host Cell Protein Assay at the Molecular Level**.

Overnight, a capture polyclonal antibody (pAb) is coated onto the surface of a 96-well plate. After blocking with BSA, the sample is then incubated (represented as purple oval) and is captured by the coating pAb. After the sample, the assay is then incubated with a biotinylated anti-HCP antibody (represented by the green antibody with blue circle). The Streptavidin conjugated Europium then binds the biotinylated antibody and is activated by the same Enhancement method as in the potency assays.

The above figure displays the molecular level binding steps that happen during each incubation presented above. Because the assay uses the same DELFIA Europium signal as the potency assays, it has a similar mechanism in which each incubation represents a new molecule adding to the scaffold, the final step of which activates the Europium signal.

2.6 Data Analysis and System Suitability

All data analysis is automated using the SoftMax Pro data analytic software (Molecular Devices, San Jose, California) for both potency assays and for the CHO HCP assay. Each assay has a dedicated SoftMax Pro template that only requires the manual input of raw data which the template then processes and automatically presents the final results.

Relative potency is calculated by first generating four-parameter logistic regression plots of each reference standard, control, and sample calculated from a plot of relative fluorescence units versus drug concentration:

$$Y = \frac{A - D}{1 + \left(\frac{X}{C}\right)^{B}} + D \qquad Equation\ 1$$

where the coefficient A is the minimum response (Y value) at the lower asymptote and D is the maximum response at the upper asymptote. The coefficient C EC_{50} is the concentration (value from the X-axis) that results in 50% of the maximal response. The coefficient B is the slope factor that describes how rapidly the curve transitions between the upper and lower asymptotes in the center of the curve. After assessing similarity, a constrained 4PL curve fit is performed and relative potency (%RP) of the drug samples is calculated by dividing the EC_{50} of the reference standard by the EC_{50} of each sample and multiplying by 100%.

In order for each potency assay to pass, the assay control must be parallel to the reference standard and must generate a relative potency between 75% and 133%; otherwise, all samples associated with that control fail and must be repeated. Individual samples must also be parallel to the reference standard to pass.

In order to be considered parallel to the reference standard, the following criteria must be met:

Table 1: **System Suitability for Potency Assays**

Reference Range	Parallelism Criteria
Lower bound, effective asymptote (D-A)	≥ 0.85
Upper bound, effective asymptote (D-A)	≤ 1.15
Lower bound, upper asymptote (D)	≥ 0.85
Upper bound, upper asymptote (D)	≤ 1.15
Slope Ratio (lower bound)	≥ 0.7
Slope Ratio (upper bound)	≤ 1.3
R-square	≥ 0.970

The host cell protein assay also uses a four-parameter logistic regression to calculate the measured impurity in each given sample. Using SoftMax Pro, a graph of relative fluorescence units versus concentration is plotted for the standard curve, which ranges in known concentrations from 4500 to 2 ng/ml. Impurity values for all samples are then calculated by interpolating the x value

concentration. Accompanying each sample is a spiked sample with a spike concentration of 250 ng/ml. The spike percent calculation is:

$$\frac{Spiked\ Sample\frac{ng}{ml} - (0.9)Non - Spiked\ Sample\frac{ng}{ml}}{Spiking\ Concentration\frac{ng}{ml}} * 100 = Spike\ Percent \quad Equation\ 2$$

3 RESULTS

The ultimate goal of the work presented in this thesis is to demonstrate the significant advantage that the collective sum of benefits of automation has to offer and to present a platform by which other similar assays may be more easily translated into an automated environment. Here, we present the results of six months of development work that produced the full automation of three assays: two relative potency assays and one residual host cell protein assay. All assays are automated using the same Hamilton Microlab STAR Liquid Handling Robot, which is customized for each assay. Regardless of the assay, each ELISA is automated from start to finish, as well as all data analysis.

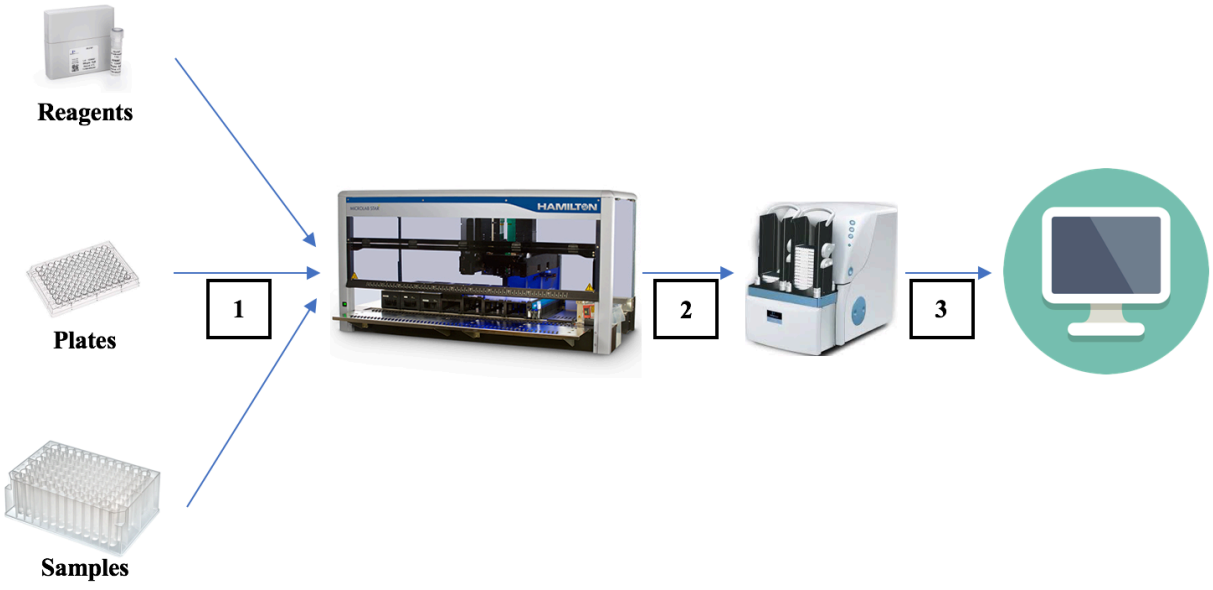

Figure 8: **Diagram of Overall General Automated Bioassay**.

For each automated assay presented in this essay, the analyst must first prepare all reagents, assay plates, and samples necessary for the assay, as well as collect all information required to give to the robot, such as desired dilution or sample concentration. These are all placed onto the deck of the robot in locations that are dictated by each assay's

corresponding program. Once the assay is begun, the assay is completely hands-off until all liquid handling steps are finished. Then, the analyst moves all assay plates to a Perkin Elmer EnVision microplate reader that reads the fluorescence. From this, the analyst copies the raw data into a pre-programmed SoftMax Pro template that automatically analyzes and reports the final results. All images come from the websites of the respective companies detailed in Materials and Methods, or from open source data.

The above diagram demonstrates the typical procedure for performing any of the assays. In order to operate, the analyst must prepare all reagents, assay plates, and samples ahead of time, as well as any data that is necessary for the robot to complete the assay. Once all materials are on the robot, all steps are automated until the end of the ELISA liquid handling, at which point the analyst removes all assay plates and measures them using a preconfigured program on a Perkin Elmer EnVision Fluorescence Microplate Reader. The analyst then copies the data into a programmed template that then automatically analyzes and reports all results.

3.1 Relative Potency Assays

In this study, we automated two relative potency assays that measure the biological activity of monoclonal antibody drugs. Potency Assay 1 measures the relative potency of Drug 1 and was developed first while Potency Assay 2 measures the relative potency of Drug 2 and was developed by modifying Potency Assay 1. Here we present data demonstrating how both assays are statistically similar to their manual counterparts. In order to evaluate each assay, we tested them for accuracy, precision, intermediate precision, linearity, and agreement. Additionally, we report other specifications of the automated assays, including total run time, analyst time, and maximum throughput.

To assess the validity of the above parameters, both potency assays tested four simulated potency samples: 60%, 77%, 130%, and 167% as well as a 100% control. All samples were tested on the new automated method as well as the qualified manual method for reference. Manually, all samples were tested a total of six times across two different analysts; on the automated platform, all samples were also tested six times across two separate runs on the same robot.

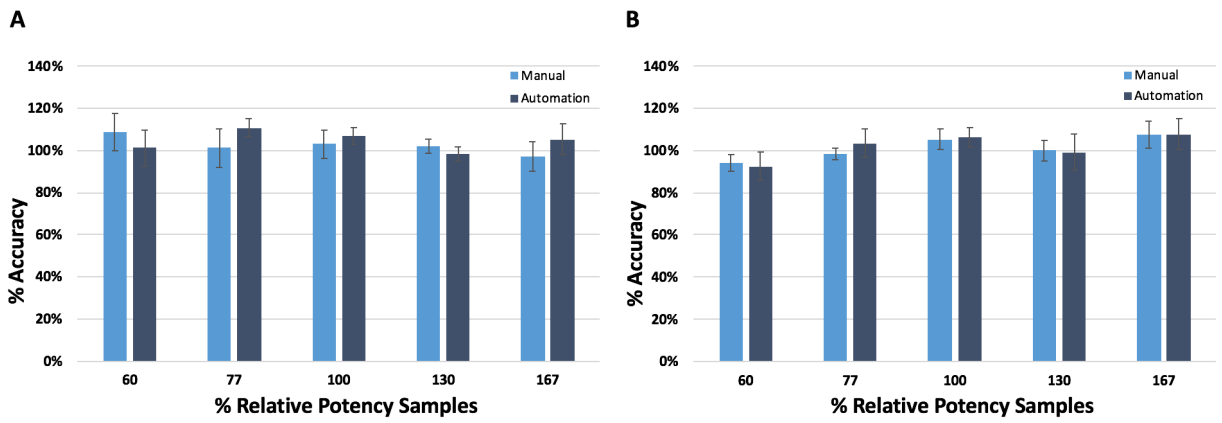

Figure 9: **Accuracy of Simulated Potency Samples**.

Accuracy is calculated by dividing the geometric mean of the observed values by the expected value and multiply by 100%. (A) Potency Assay 1 (B) Potency Assay 2.

The above data in Figure 9 represents the accuracy of each simulated sample for both the manual and automated versions of both relative potency assays. Across all assays, both manual and automated, the maximum range of accuracy does not extend beyond 92% – 111.

Precision of each assay was evaluated for intra-assay precision as well as overall assay precision.

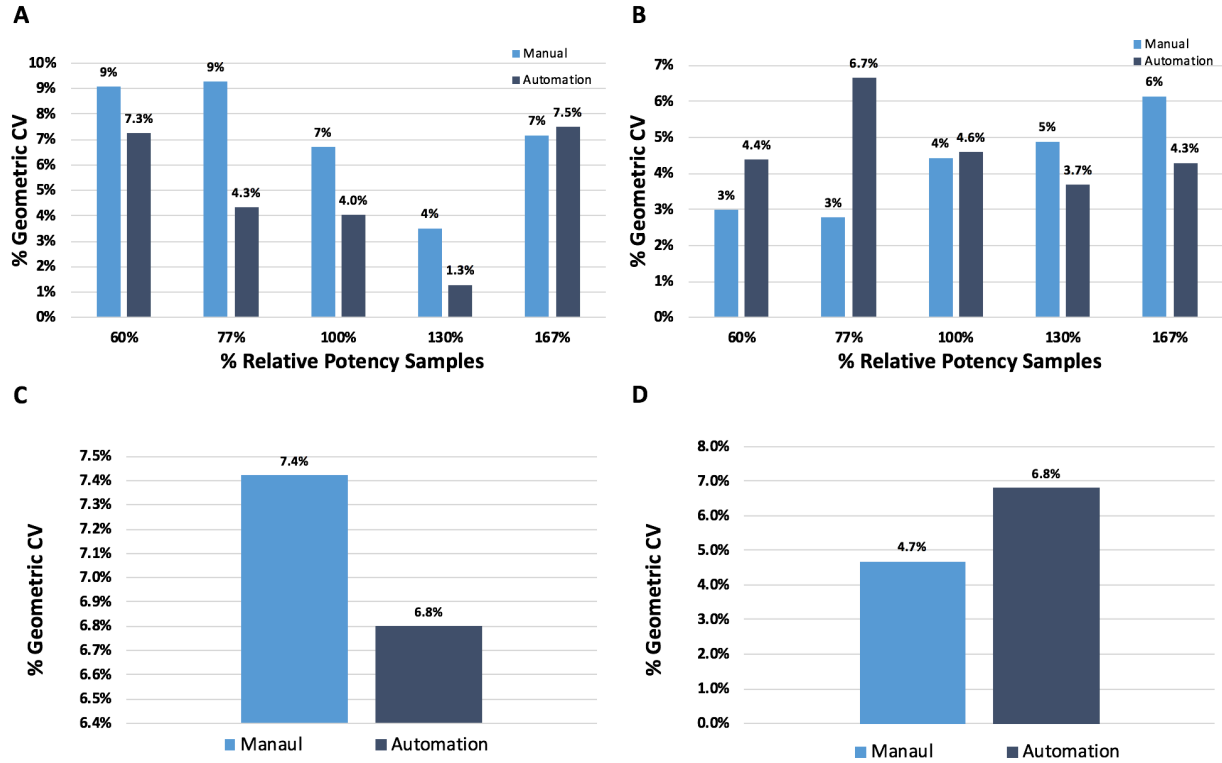

Figure 10: **Precision of Simulated Potency Samples**.

(A) Intermediate Precision per Level Potency Assay 1 (B) Intermediate Precision per Level Potency Assay 2 (C) Overall Intermediate Precision Assay 1 (D) Overall Intermediate Precision Assay 2.

Figures 10 A-D demonstrate the precision of both potency assays. Figures 10A and 10B represent the intra-assay precision, or repeatability, of each simulated potency sample and are calculated by determining the % geometric coefficient of variation across all six tests for all simulated samples, both manual and automated. Individual sample % geometric CV was calculated by the following equation:

$$\%\ Geometric\ CV = \exp\left(\sqrt{Mean\ Squared\ Error}\right) - 1 * 100\% \quad Equation\ 3$$

Overall intermediate precision was calculated similarly by using the arithmetic mean of the total five mean squared errors for each simulated sample. For Potency Assay 1, the automated assay has consistently smaller CVs than that of the manual method, while Potency Assay 2 more closely agrees with its manual counterpart (bar the 77% sample that is higher). Additionally, Figures 10C and 10D demonstrate the similarity between the overall precision of the manual and automated assays. Furthermore, across all assays, CVs did not exceed 10%, demonstrating that each automated assay maintains the overall precision of their manual counterparts.

To further assess the overall quality of the automated assays developed, we calculated the linearity of the simulated samples, ranging from 60% to 167%.

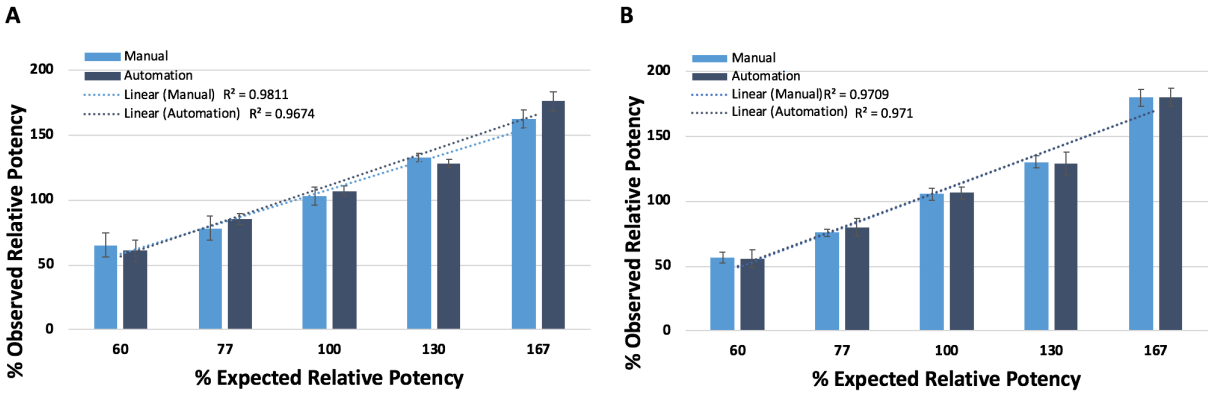

Figure 11: **Linearity of Simulated Samples**.

The geometric mean of all simulated samples within each assay is plotted as the observed potency against its corresponding expected potency. (A) Potency Assay 1 (B) Potency Assay 2.

As seen in the above figure, all simulated samples across all assays demonstrate a strong linear relationship throughout the tested range, with all R^2 values well above 0.95. Furthermore, each automated assay has significantly similar R^2 values to its manual counterpart, demonstrating that our automated assay maintains the linear integrity of the existing assays. This well-preserved linearity demonstrates that the automated methods developed in this study can reliably measure a given sample for its relative potency within this region of values.

Finally, the automated methods were tested for agreement with the manual methods with which we aim to replace them. While the linear relationship presented above demonstrates a strong correlation between the manual and automated methods, it does not account for agreement between them. Commonly used for assessing the agreement between two methods that measure the same parameter, the Bland-Altman plot in Figure 12 below represents the ratio of means of manual versus automated methods (mean observed manual potency / mean observed automated potency). The mean ratios for each assay, 0.981 and 0.994, respectively, demonstrate that the two methods on average return near identical results for a given sample. All averaged simulated samples fall within two standard deviations and the standard error for each sample also predominantly remains within two standard deviations, demonstrating the agreement between the two assays.

The distribution trend between the two assays is also worth noting. For four out of the five simulated samples, the ratios of means are skewed in the same direction across both assays. For example, the reported ratio for the 60% simulated sample is slightly over 1.0 while it is slightly under that for the 77% sample across both assays, indicating that the automated method produces lower and higher results for each sample, respectively. While the values of each sample are not significant and seem to be distributed normally, the striking resemblance in the trends between the two assays suggests that there is potentially a noticeable difference between the automated platform and the manual.

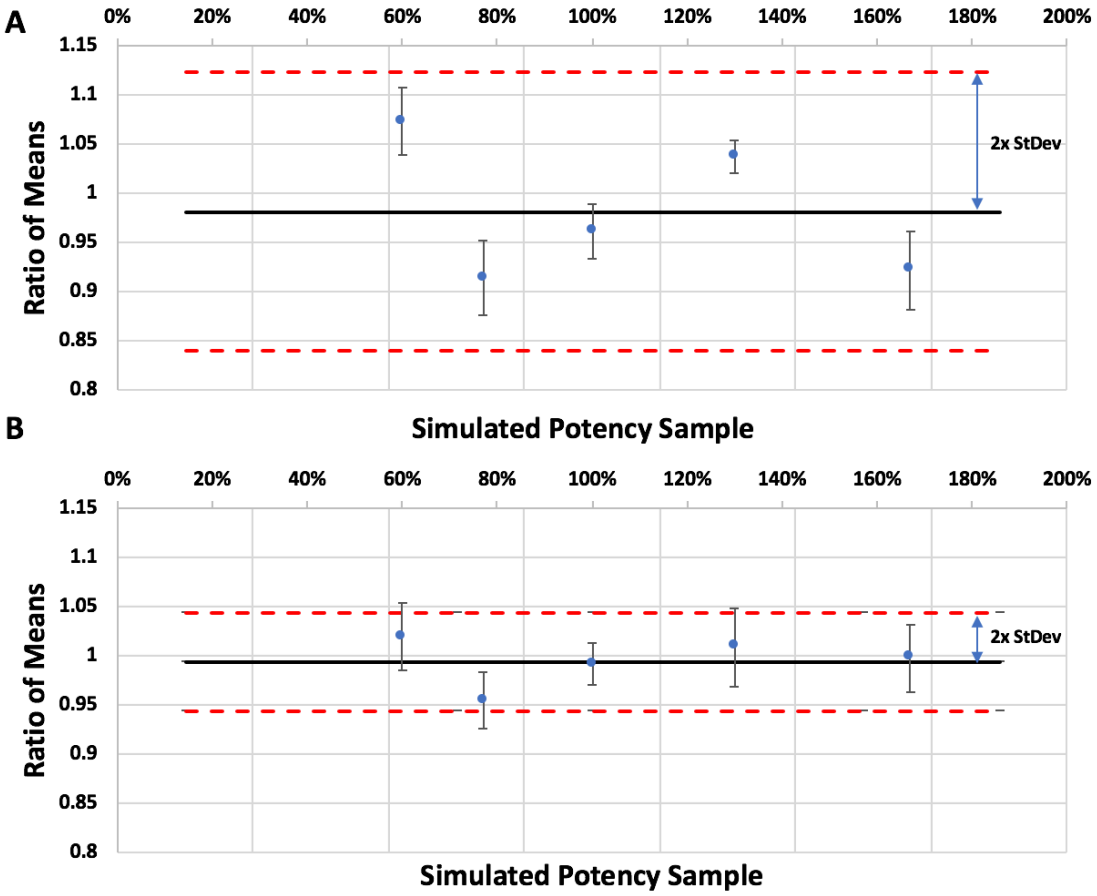

Figure 12: **Ratio of Means of Manual vs. Automated Methods**.

The solid black line represents the average of all samples from the manual assays divided by that of the automated assays. Each data point represents the ratio of the mean of each simulated manual sample divided by each automated sample, including bars for standard error. The dashed red lines represent two times the standard deviation. (A) Potency Assay 1: The mean is 0.981 and two times the standard deviation is 0.14. (B) Potency Assay 2: The mean is 0.994 and two times the standard deviation is 0.05.[4,5]

For both automated assays, each program can be completed in under 5 hours. Excluding the cell culture preparation the day prior which should take no longer than 30 minutes, analyst time the day of the assay does not exceed 30 minutes, reducing total analyst time to under an hour over two days. Each assay can accommodate a maximum of 12 samples. In comparison, an analyst can comfortably do only 4 samples at a time, which would take up the majority of the analyst's day.

3.2 Residual CHO Host Cell Protein Assay

The third assay presented in this essay is an assay to measure residual CHO host cell protein in development drug samples that, in contrast to the previous assays that were automated versions

of their manual counterparts, was developed and automated simultaneously. The assay was developed from its original ELISA version that used the traditional horseradish peroxidase (HRP) enzyme. The HRP enzyme catalyzes the oxidation of numerous substrates that, when oxidized, change color. Thus, it has been used in a conjugated form very effectively as a method of detection in ELISAs using relatively inexpensive spectrophotometer instruments. However, its rapid reaction rates as well as its relative instability make it an undesirable candidate for high-throughput automation. Therefore, in this study, we adapted the existing manual CHO host cell protein ELISA to use Perkin Elmer's DELFIA Europium, with which we have previously demonstrated success in automation, in lieu of the HRP enzyme and its corresponding substrate. Simultaneously, we developed an automated method using the Hamilton Microlab STAR that can accommodate up to 36 samples. At its maximum capacity, the assay takes six and a half hours to run on the robot with a total manual time of 45 minutes, bringing the assay to a total of just over seven hours, easily achievable within the 8-hour workday.

In addition to increased stability and therefore its availability for use in an automated environment, the use of Perkin Elmer's fluorescent Europium chelate has other significant advantages.

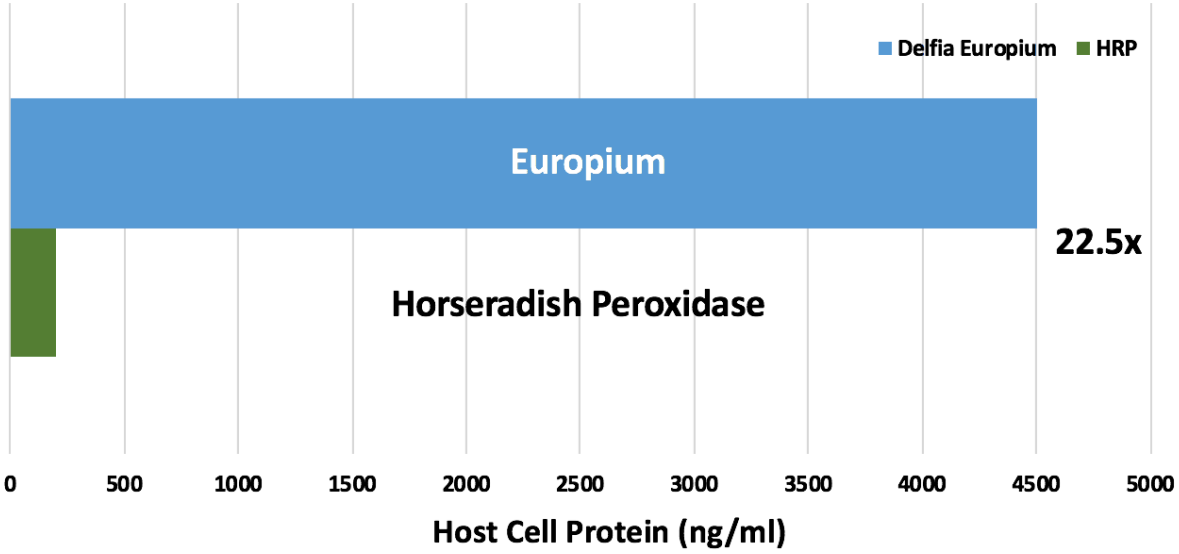

Figure 13: **Dynamic Range of HCP Assays**.

DEFLIA Europium Chelate vs. Horseradish Peroxidase reaction with ABTS. By using Europium rather than the HRP enzyme, our assay can accommodate a dynamic range 22.5 times as large as the HRP's range.

The above figure demonstrates the difference in standard curve range between the two assays: the use of Europium increases the dynamic range of the assay by more than 22-fold, dramatically increasing the range of impurity concentrations that the assay can accurately detect. Because the impurity concentration is unknown before the assay is run, having a wider dynamic range results in a greater chance that the impurity concentration can be identified, decreasing the number of samples that need to be retested. In addition to increased range, the Europium allows for a more linear standard curve leading to a more overall proportional assay.

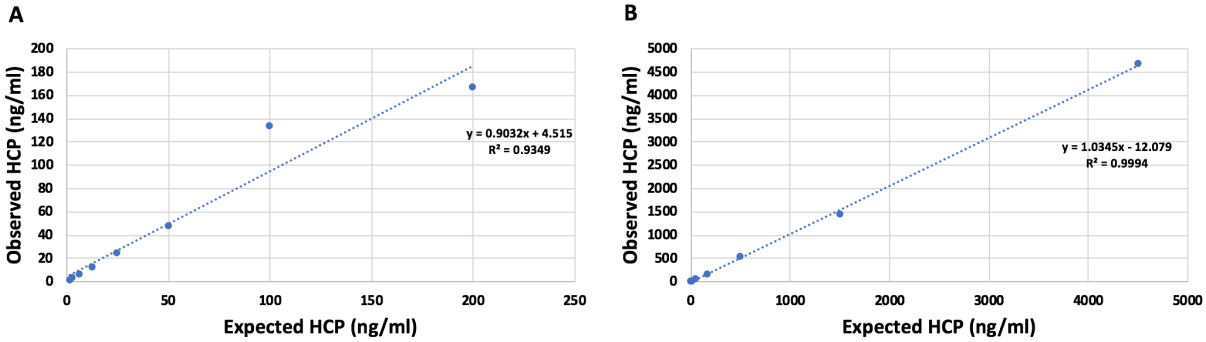

Figure 14: **Linearity of Standard Curves**.

Observed and expected values of host cell protein are plotted against each other for each value of the standard curve in (A) the HRP and ABTS substrate assay and in (B) the Europium assay.

The data above were taken from two independent runs of both assays in which the standard curves of known host cell protein concentration of both assays were plated in triplicate and duplicate for the HRP and Europium assays, respectively, and each value of the curves was then processed to determine their recovered values for HCP impurity. The graphs above show the observed values of host cell protein concentration in each point of both standard curves that each assay recovered in comparison to the expected values calculated from dilutions of known concentrations of stock host cell protein. The Europium ELISA demonstrates improved linearity as well as a slope closer to unity than the HRP assay. The increased linearity shows that the Europium assay is more consistent throughout its range and its slope of 1.03 demonstrates its overall improved accuracy over the HRP assay, with a slope of 0.90.

To further assess the performance of the newly developed CHO residual host cell protein assay, we tested each point of the standard curve as simulated samples plated in triplicate across four different manual trials. The data are collected in the table below:

Table 2: **Europium Standard Curve Tested as Simulated Samples**

Expected HCP (ng/ml)	Observed HCP (ng/ml)	% Accuracy	%CV	% Standard Error
4500	5423.2	120.5%	17.9%	11%
1500	1312.8	87.5%	12.7%	6%
500	492.5	98.5%	17.3%	9%
166.7	163.0	97.8%	22.1%	11%
55.6	49.7	89.5%	13.4%	6%
18.5	18.1	97.8%	14.1%	7%
6.2	7.3	117.6%	5.2%	3%
2.1	4.5	218.4%	30.0%	33%

The above data were analyzed for accuracy, precision, and linearity. The figure below shows the accuracy and precision of the assay according to each sample within the standard curve.

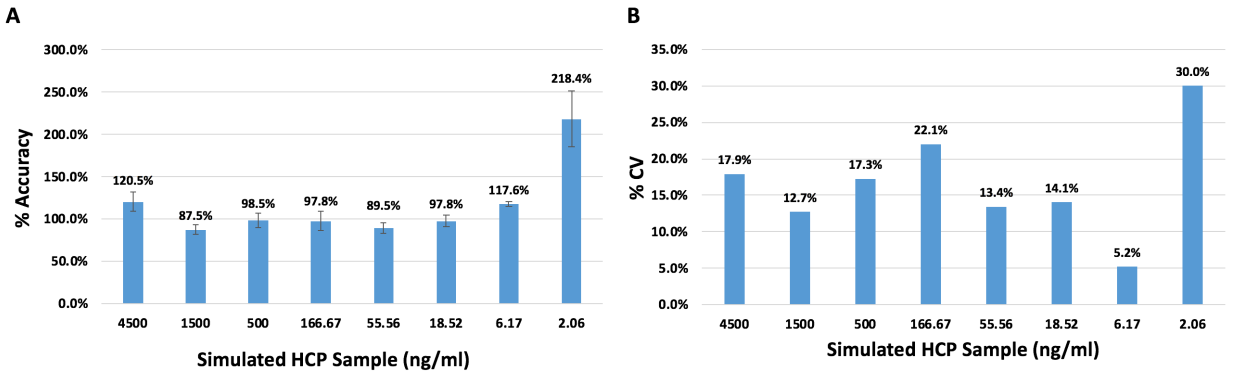

Figure 15: **Accuracy and Precision of the Manual Europium HCP Assay**.

(A) Accuracy (B) Precision, represented by the %CV of each simulated sample.

The above data show that the majority of the concentrations in the standard curve can be recovered with both good accuracy and precision. In between 6 ng/ml and 1500 ng/ml, the assay can accurately report the simulated concentrations within 17% above and 13% below the target with an average % CV of 14.1%, which falls under the 15% typically used as a benchmark. Furthermore, the assay demonstrates strong linearity.

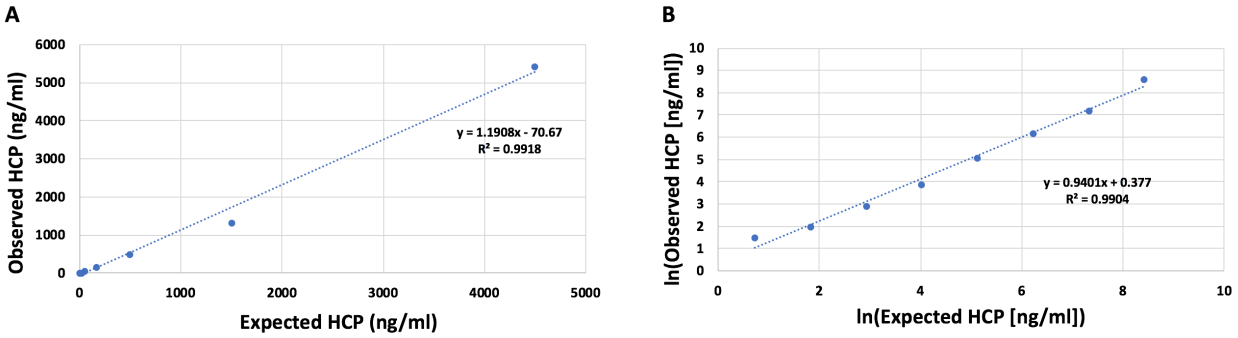

Figure 16: **Linearity of Manual Europium HCP Assay**.

(A) The observed versus expected HCP values are plotted without modification compared to (B) The natural log is taken of each individual value and graphed separately due to the exponential nature of the standard curve.

Figures 16A and 16B above demonstrate the assay's linearity across all simulated HCP samples of the standard curve. The data were analyzed for linearity by comparing the observed HCP found by the assay to the expected concentration without alteration as well as modifying the data set by taking the natural logarithm due to the standard curve's exponential nature. Both methods report an R^2 value above 0.99 as well as a slope close to unity. The linear nature of the assay we have developed in this study demonstrates its ability to recover proportional results throughout the range of the standard curve.

While the assay recovers simulated samples in the middle of its range well, it is more variable at the topmost and bottommost ends of the range. This is normal for an assay of this nature; however, in order to better understand our assay, we conducted a study to evaluate the upper and lower limits of quantification for this assay. Therefore, we performed a series of experiments that tested simulated samples at the lower and upper end of the curve. The experiments tested nine simulated HCP samples three separate times in four 1:2 dilutions and in duplicate using the automated method we developed on the Hamilton Microlab STAR.

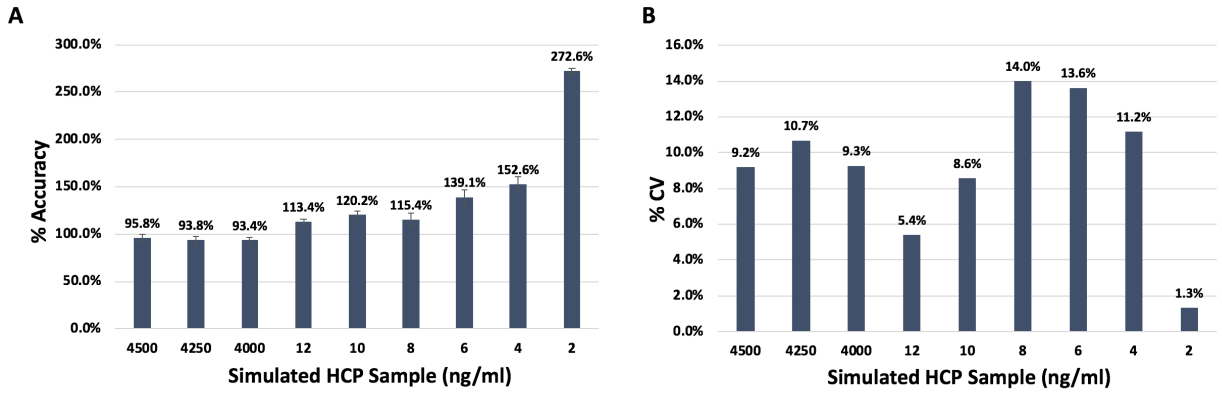

Figure 17: **Accuracy and Precision of Upper and Lower Limits of Automated HCP Europium Assay**.

(A) Accuracy of simulated samples from upper (4500, 4250, and 4000 ng/ml HCP) and lower limits (12, 10, 8, … 2 ng/ml HCP) of the standard curve. (B) Precision of each simulated sample reported as %CV.

The above figure shows the accuracy and precision of all nine simulated samples across all trials: the first three samples that tested the upper limit of quantification demonstrate both accuracy and precision. In comparison to Figure 15 that showed insufficient accuracy and precision for the 4500 ng/ml simulated host cell protein sample, these data demonstrate otherwise, most probably because these simulated samples are tested in a series of dilutions. The series of 1:2 dilutions is standard on the assay in order to achieve a greater chance of obtaining a result within the working range outlined in Figure 13. The following six simulated samples that tested the lower region see a decrease in accuracy as the series of dilutions begin to negatively affect the assay results due to the lower limit of quantification. The data presented above suggest that 6 ng/ml is the lower limit of quantification, yet further work is required to statistically prove this.

The series of 1:2 dilutions as well as the automation made significant improvements to the data presented; to better understand the performance of the dilutions themselves, we analyzed the data from the three simulated samples that tested the upper limit of quantification (because the lower simulated samples' dilutions result in concentrations below the level of quantification). The three simulated samples, 4500, 4250, and 4000 ng/ml HCP, were analyzed by their individual dilutions, normalized, and plotted against their normalized expected concentrations in the figure below.

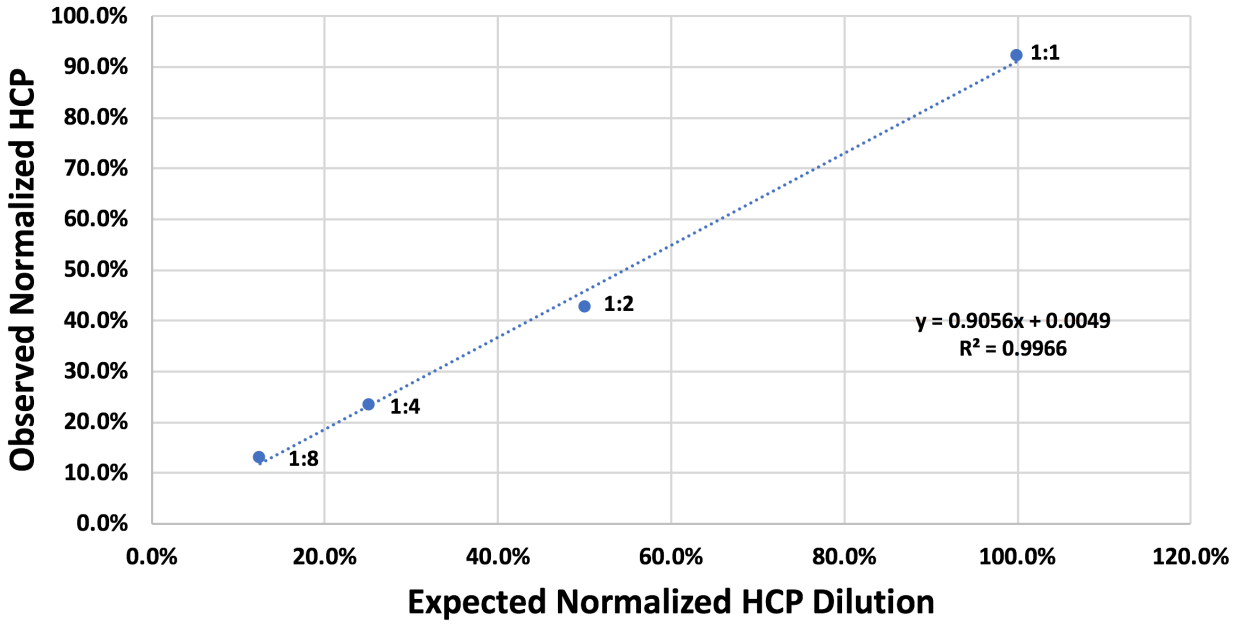

Figure 18: **Normalized Linearity of 1:2 Dilutions**.

The data plotted above shows the linearity of the 1:2 dilutions (1:2, 1:4, and 1:8, as well as the original 1:1) for the three samples that tested the upper limit of the standard curve: 4500, 4250, and 4000 ng/ml. Lower samples were not used since the lowest dilutions will not fall within the lower limit of the assay. Since concentrations for each sample come from different initial simulated samples, values were normalized to the percentage that each dilution should represent (i.e., 1:1 should be 100%, 1:2 50%, etc.).

The linearity observed in the data in Figure 18 (R^2 is 0.997) demonstrates that the robot dilutes all samples properly and the assay can accurately return values of all dilutions that still fall within the range of the quantification. The slope slightly below 1.0 in the above figure is most likely the result of the concentrations of the first dilution (1:1) being near to the upper limit of the assay.

The final aspect of our newly developed host cell protein assay that we tested evaluated the assay's ability to recover a simulated host cell protein sample in the presence of known impurities likely to be found in typical samples, including CHO Protein A, Insulin, and DNA. We performed experiments in which a known concentration of CHO HCP antigen was tested by our assay in the presence of a known concentration of the above impurities, data for which is presented below on both the manual and automated methods.

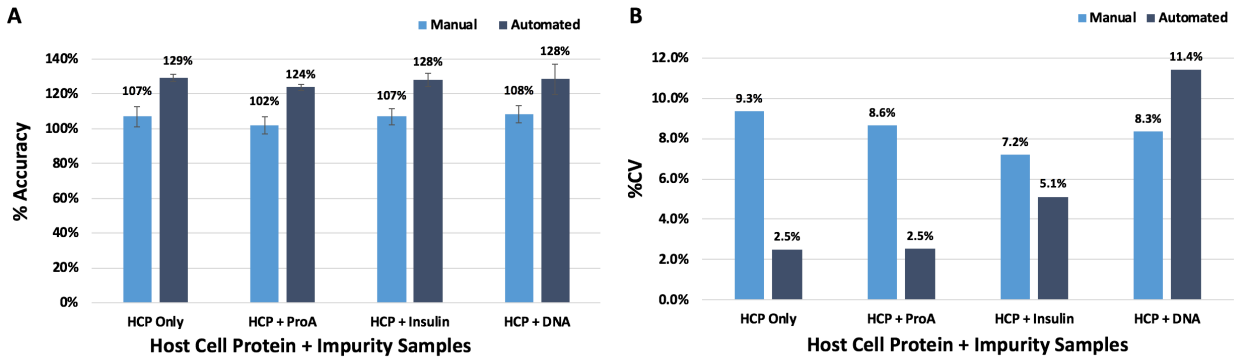

Figure 19: **Accuracy and Precision of Simulated HCP Samples with Additional CHO Impurities**.

Each simulated sample was tested three times on each method, manual and automated. All samples contain 250 ng/ml of HCP. HCP + Pro A samples contain 30 ng/ml of residual Protein A, HCP + Insulin samples contain 50 µIU/ml of residual Insulin, and HCP + DNA samples contain 30 ng/ml of residual CHO DNA. (A) Accuracy of all samples and (B) Precision of all samples represented as %CV.

The data above suggest that the newly developed assay using Europium is unaffected by the presence of other residual impurities. Accuracy values for both the manual and automated assays maintain their consistency across the different impurity samples. There is, however, a significant difference in accuracy between the manual and automated versions of the assay. While the manual assay is more consistently accurate than the automated assay, the automated assay is overall more precise. One way to rationalize this result is that the robot, while able to pipette very precisely, is programmed in a manner that resulted in an overshoot in recovering known sample concentrations. While these data demonstrate that both assays can function effectively in the presence of the most common impurities external to the assay objective, more experiments should be performed to test the robustness of the automated method's dilution accuracy.

4 DISCUSSION AND FUTURE DIRECTIONS

The automated assays presented in this thesis have significant advantages over their manual counterparts, and even more potential advantages that have yet to be explored. Our assays have completely automated ELISA procedures as well as automated preparatory dilutions and data analysis. Automation of sample dilutions is in particular important for the residual host cell protein assay, in which the dilutions can vary between 2 and 2000-fold from sample to sample and run to run with no predictable pattern. The automation of both the dilutions and their corresponding calculations affords the analyst not only the convenience of not having to manually perform liquid

handling tasks but also completes them dramatically faster than an analyst could manually. At the manual rate, an analyst could not calculate and perform all dilutions for an equivalent maximum capacity compared to the automated protocol while also completing the assay within the workday, making the automation of sample dilutions as well as their calculations one of the best advantages that the automated protocol offers. Furthermore, we have demonstrated that automated assays can achieve equal or superior accuracy and precision over their manual counterparts. Additionally, every assay in this essay automatically generates a file that records every movement of the robot, providing more accountability than with a manual assay.

In addition to the successes outlined above, there are a series of steps that can dramatically improve these bioassays with more development. One addition that we explored but did not finish during this study is the addition of a barcode to each assay plate that can be read by both the liquid handling robot as well as the microplate reader and then subsequently be fed into the analytical software. Because each sample is already coded within an existing system and the liquid handling robot comes equipped with a barcode reader, a barcode on each plate would allow for complete automation of the assay, including data analysis, from the point that the samples enter the robot to the final sample result.

Additionally, a step missing from the assays developed here that significantly limits their operation is the robotic transfer of plates to the microplate reader, which currently happens manually. The automation of this step is not complex and involves placing a dedicated microplate reader next to the liquid handling robot and connecting the two with a communication pathway. Theoretically, the robot could use its already existing arm to place each plate on the reader that would then use the barcode mentioned above to direct the microplate reader to operate the appropriate program with which to read the plate and then subsequently open the correct analytical software to process and analyze the raw data. These two additions are critical to automating the bioassays from the beginning of the assay to the final result. This is not only advantageous for all the reasons listed throughout this essay, but it would also enable the assay to be operated twice as often: once that begins and ends during business hours and a second that starts at the end of business hours and finishes after they conclude. These two additions could effectively double the efficiency of the assays presented in this essay.

While each assay presented here is a success in and of itself, the developmental work done to create them establishes successful methods for overcoming many of the hurdles one faces when

replacing manual assays with automated assays. A series of environmental differences between a manual and automated setting that dictate what can and cannot be done during an automated assay were tested such that automation adaptation could be feasible. These include differences such as protecting the assays from light, plate wash protocols, and the use of plate shakers. While all of the above factors are easily controlled by a human, an automated robot cannot adjust for these without the proper intelligence and mechanical equipment. For example, all manual plate washing protocols call for using the BioTek plate washer followed by tapping the 96-well microtiter plate onto non-shredding paper towels, which is not feasible for a robot to do. By developing robust methods for circumventing these hurdles, we have established a precedent that will streamline further automation.

In addition to achieving complete automation, there are many aspects of the assays presented here whose altering would improve their overall robustness. For example, while the host cell protein assay can accommodate up to 36 samples, the assay could be modified to instruct the user to only supply the robot with the amount of reagents needed for the particular number of samples it needs to run. This would involve putting the assay through a battery of tests to determine exactly how much is needed for each condition.

The power of automation is easily seen from the work presented in this essay, as well as from the advances it has produced across different industries. However, there are problems that still exist in the assays developed here, as well as inherent weaknesses of automation that are more challenging to overcome. For example, the Hamilton robot is less skilled at aspirating liquid from very small volumes. The Hamilton Microlab STAR is equipped with advanced technologies that use conductance to detect liquid surface levels, but depending on the amount of liquid, the vessel shape and size, and the viscosity of the liquid, it can be more or less effective. In contrast, a trained human analyst with a microcentrifuge tube with only a few microliters of liquid can easily observe the liquid level and almost always pipette correctly. This artifact of the robot results in its overconsumption of reagents, which are especially expensive when using Perkin Elmer's DELFIA reagents that are used throughout this study. In addition to purchased reagents, critical reagents that are made and qualified in-house are significantly more precious and their over-consumption presents a potential problem due to the difficulty of remaking and requalifying a new batch of critical reagent, which would affect many departments throughout the business. Another

consequence of the robot's limitation is that it will occasionally pipette air bubbles and not report an error, completing the assay incorrectly and yielding inaccurate or incomprehensible results.

Furthermore, the assays developed here suffer from non-recoverable robotic errors. If an error occurs, such as a pipette not being able to secure a pipette tip correctly or a miscommunication between the robot and the plate washer, both of which are not uncommon, the robot has a limited ability to resolve the issue on its own, requiring manual intervention. Moreover, in order to even have options to resolve such issues, every scenario that could result in an error must be predicted in order for the robot to be intelligent enough to know what to do in the event of an error. However, even manual intervention is often not sufficient to resolve the issue. Because the assays cannot be started from midway through the experiment without altering the robot's code, the assay becomes unrecoverable, losing both time, reagents, and samples.

5 CONCLUSION

The work presented in this thesis highlights the benefits, as well as the potential weaknesses, of integrating customizable automated liquid handling into routine analytics in biopharmaceuticals. Yet, regardless of its potential pitfalls, the ultimate reality is that in order for biotechnology companies to remain competitive and to maintain efficiency with an evergrowing analytical demand, the incorporation of automation is necessary. The work presented here demonstrates significant strides for the immediate yet limited incorporation of automation into the everyday lives of analytical sciences. We have yet to see the full capability of customizable liquid handling robots, and their future development is very bright.

6 REFERENCES

1. Baden-Württemberg GmbH. (2013, March 25). Biotechnology Goes Automated. Retrieved June 1, 2018, from www.gesundheitsindustrie-bw.de
2. Ecker, D. M., Jones, S. D., & Levine, H. L. (2014). The therapeutic monoclonal antibody market. *MAbs, 7*(1), 9-14. doi:10.4161/19420862.2015.989042
3. Konstantinidis, S., Kong, S., & Titchener-Hooker, N. (2013). Identifying analytics for high throughput bioprocess development studies. *Biotechnology and Bioengineering, 110*(7), 1924-1935. doi:10.1002/bit.24850
4. Giavarina, D. (2015). Understanding Bland Altman analysis. *Biochemia Medica, 25*(2), 141-151. doi:10.11613/bm.2015.015
5. Rey, G., & Wendeler, M. W. (2012). Full automation and validation of a flexible ELISA platform for host cell protein and protein A impurity detection in biopharmaceuticals. *Journal of Pharmaceutical and Biomedical Analysis, 70*, 580-586. doi:10.1016/j.jpba.2012.05.027

Author's Note: All images presented in this essay that are not original creations of the author are taken from either the websites of companies from which we purchased materials, which are listed in the Materials and Methods section, or they are from open sources without copyright. All original figures were created using Microsoft Office, Apple's Preview, or a combination of the two, including all 96-well plates, diagrams, and data.

7 APPENDIX: SUPPLEMENTAL DATA

The data presented in the body of this thesis represents the evaluation of months of development work into the three corresponding assays, not to mention extensive troubleshooting. The following section supplies some of the most significant development studies in addition to exact numbers represented in results figures for reference.

Table 3: **Drug Potency Assay 1 Data**

Simulated Potency Sample	60%	77%	100%	130%	167%
Geometric Mean Manual	65%	78%	103%	133%	162%
Geometric Mean Automation	61%	85%	107%	128%	176%
% Accuracy Manual	109%	101%	103%	102%	97%
% Accuracy Automation	101%	111%	107%	98%	105%
Repeatability (%GCV) Manual	9.1%	9.3%	6.7%	3.5%	7.2%
Repeatability (%GCV) Automation	7.3%	4.3%	4.0%	1.3%	7.5%
Ratio of Means	1.073	0.914	0.962	1.037	0.922

Table 4: **Drug Potency Assay 2 Data**

Simulated Potency Sample	60%	77%	100%	130%	167%
Geometric Mean Manual	57%	76%	105%	130%	179%
Geometric Mean Automation	55%	80%	106%	129%	180%
% Accuracy Manual	94%	99%	105%	100%	107%
% Accuracy Automation	92%	103%	106%	99%	108%
Repeatability (%GCV) Manual	3.0%	2.8%	4.4%	4.9%	6.2%
Repeatability (%GCV) Automation	4.4%	6.7%	4.6%	3.7%	4.3%
Ratio of Means	1.019	0.954	0.991	1.009	0.998

The above tables are the exact numbers for Figures 9-12

Perhaps the most important study performed for the development of the work presented in this essay is the establishment of a new residual HCP assay. While the drug potency assays were automated versions of existing manual assays, the residual HCP assay was a newly designed

ELISA. With a series of components to work with, we completed a design of experiment in order to best determine the operating conditions of many of the components in the assay.

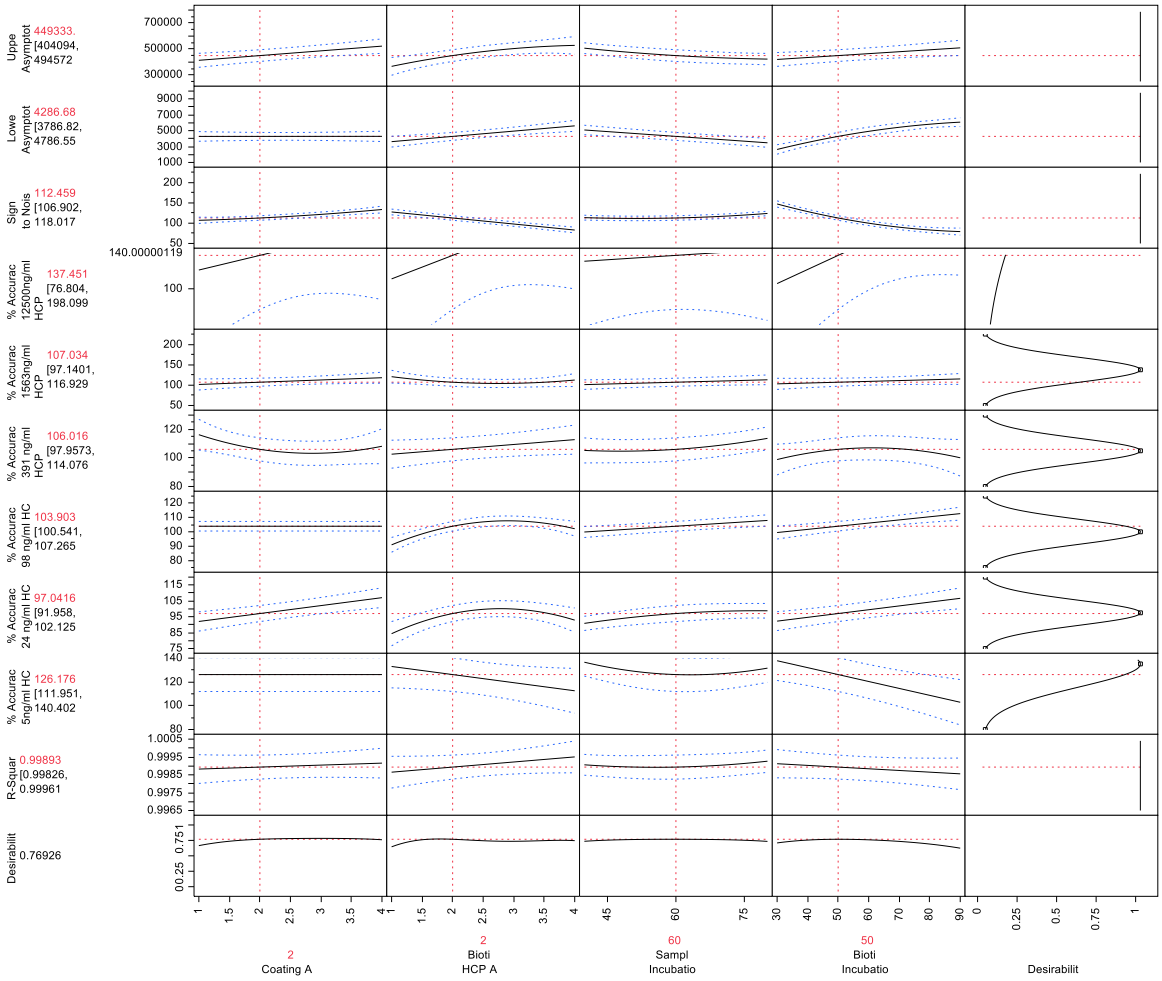

Figure 20: **DOE for Establishing a Residual CHO HCP Assay using DELFIA Europium**.

The above data shows the results from our DOE that tested the following assay variables: coating polyclonal antibody concentration, biotinylated antibody concentration, sample incubation time, and biotinylated antibody incubation time. The data presented above comes from a total of 52 combinations of the previously listed variables at different values in between what is shown on the figure's x-axis. This experiment was critical in our determination of the final variables that are explicitly described in the Materials and Methods section. One of the most critical components of the above study was the sample incubation time. Because of the way the automated protocol plated samples into and washed each of the nine assay plates, it was critical that the sample incubation time not affect the final sample results between 40 and 80 minutes, which is well demonstrated in the desirability graph for sample time incubation in Figure 20.

BIOGRAPHY

Joseph Federico was born in 1994 in southern New Hampshire. In 2013, Joseph began his undergraduate studies at The Johns Hopkins University where he received a Bachelor of Science in Chemical and Biomolecular Engineering with a concentration in Cellular and Molecular Biology and a minor in French. In addition to his course curricula, Joseph participated in academic research, studying regenerative medicine in the lab of Dr. Sharon Gerecht for three years as well as becoming a brother in the professional business fraternity, Alpha Kappa Psi. In addition to academic research, Joseph spent multiple summers applying his education in a series of internships, including companies Becton Dickinson and Biogen. He also spent three years tutoring in the subjects of cell biology and biochemistry in addition to managing the tutoring program himself.

Joseph received a series of honors and awards during this time, including both university and departmental honors, the Sarah K. Doshna Undergraduate Research Award, and the Morton J. and Louise D. Macks Endowed Scholarship, as well as being inducted in the Engineering Honor Society, Tau Beta Pi.

In 2017, Joseph continued at the Johns Hopkins University to pursue his Master of Science in Engineering in Chemical and Biomolecular Engineering, in which he performed the research for his degree at the biotechnology leader, MedImmune, a wholly owned subsidiary of AstraZeneca in Gaithersburg, Maryland.